

# Optical forces in coupled plasmonic nanosystems: Near field and far field interaction regimes

Élodie Lamothe, Gaëtan Lévêque, and Olivier J. F. Martin

*Nanophotonics and Metrology Laboratory  
Swiss Federal Institute of Technology  
EPFL-STI-NAM, ELG, Station 11  
CH-1015 Lausanne, Switzerland*

[elodie.lamothe@epfl.ch](mailto:elodie.lamothe@epfl.ch)  
[gaetan.leveque@epfl.ch](mailto:gaetan.leveque@epfl.ch)

<http://www.nanophotonics.ch/>

**Abstract:** We study the forces generated by an electromagnetic field on two coupled gold nanowires at the vicinity of the plasmon resonance wavelength. Two different regimes are observed, depending on the separation distance  $d$  between the wires. In the near field coupling regime, both attractive and repulsive forces can be generated, depending on  $d$  and the illumination wavelength. Furthermore, at the plasmon resonance, it is possible to create forces 100 times larger than the radiation pressure. In the far field coupling regime, both particles are pushed by the incident field. However, the force amplitude applied on each wire is modulated as a function of  $d$ , even for large separations. This indicates that the system behaves like a cavity and pseudo Fabry-Perot modes can be excited between the particles. The interaction of these modes with the plasmon resonances of the nanowires, determines the forces on the particles. Around the plasmon resonance wavelength, when the cavity is tuned to the incident light, forces are close to the average value corresponding to the radiation pressure of the incident field. On the other hand, when the cavity is detuned, the particles are retained or pushed anti-symmetrically. We finally study the forces applied on these nanowires in the centre of mass reference frame (CMRF) for the far field coupling regime. For any separation distance  $d$  we observe equilibrium positions in the CMRF for at least one illumination wavelength. The stability of these equilibrium positions is discussed in detail.

©2007 Optical Society of America

**OCIS codes:** (240.6680) Surface plasmons; (020.7010) Trapping; (170.4520) Optical confinement and manipulation; (290.290) Scattering.

---

## References and links

1. H. Raether, *Plasmons on Smooth and Rough Surfaces and on Gratings* (Springer-Verlag, Berlin, 1988).
2. J. P. Kottmann, O. J. F. Martin, D. R. Smith, and S. Schultz, "Plasmon resonances of silver nanowires with a nonregular cross section," *Phys. Rev. B* **64**, 235402 (2001).
3. G. Lévêque and O. J. F. Martin, "Optical interactions in a plasmonic particle coupled to a metallic film," *Opt. Express* **14**, 9971-9981 (2006).
4. A. Ashkin, "Acceleration and trapping of particles by radiation pressure," *Phys. Rev. Lett.* **24**, 156-159 (1970).
5. A. Ashkin, J. M. Dziedzic, J. E. Bjorkholm, and S. Chu, "Observation of a single-beam gradient force optical trap for dielectric particles," *Opt. Lett.* **11**, 288-290 (1986).
6. A. Ashkin, "Trapping of atoms by resonant radiation pressure," *Phys. Rev. Lett.* **40**, 729-732 (1978).
7. M. M. Burns, J. M. Fournier, and J. A. Golovchenko, "Optical binding," *Phys. Rev. Lett.* **63**, 1233-1236 (1989).

8. C. Girard, A. Dereux, and O. J. F. Martin, "Theoretical analysis of light-inductive forces in scanning probe microscopy", *Phys. Rev. B* **49**, 13872-13881 (1994).
9. P. C. Chaumet, and M. Nieto-Vesperinas, "Coupled dipole method determination of the electromagnetic force on a particle over a flat dielectric substrate," *Phys. Rev. B* **61**, 14119-14127 (2000).
10. P. C. Chaumet, and M. Nieto-Vesperinas, "Electromagnetic force on a metallic particle in the presence of a dielectric surface," *Phys. Rev. B* **62**, 11185-11191 (2000).
11. M. L. Povinelli, M. Lončar, M. Ibanescu, E. J. Smythe, S. G. Johnson, F. Capasso, and J. D. Joannopoulos, "Evanescent-wave bonding between optical waveguides," *Opt. Lett.* **30**, 3042-3044 (2005).
12. R. Gómez-Medina, and J. J. Sáenz, "Unusually strong optical interactions between particles in quasi-one-dimensional geometries," *Phys. Rev. Lett.* **93**, 243602 (2004).
13. L. Novotny, R. X. Bian, and X. S. Xie, "Theory of Nanometric Optical Tweezers," *Phys. Rev. Lett.* **79**, 645-648 (1997).
14. P. Chaumet, A. Rahmani, and M. Nieto-Vesperinas, "Selective nanomanipulation using optical forces," *Phys. Rev. B* **66**, 195405 (2002).
15. J. R. Arias-Gonzalez, and M. Nieto-Vesperinas, "Optical forces on small particles: attractive and repulsive nature and plasmon resonance conditions," *J. Opt. Soc. Am. A* **20**, 1201-1209 (2003).
16. K. Halterman, J. M. Elson, and S. Singh, "Plasmonic resonances and electromagnetic forces between coupled silver nanowires," *Phys. Rev. B* **72**, 075429 (2005).
17. A. S. Zelenina, R. Quidant, and M. Nieto-Vesperinas, "Enhanced optical forces between coupled resonant metal nanoparticles," *Opt. Lett.* **32**, 1156-1158 (2007).
18. P. B. Johnson and R. W. Christy, *Phys. Rev. B* **6**, 4370-4379 (1972)
19. J. A. Stratton, *Electromagnetic Theory* (McGraw-Hill, New York, 1941).
20. M. Paulus, and O. J. F. Martin, "Green's tensor technique for scattering in two-dimensional stratified media," *Phys. Rev. B* **63**, 066615 (2001).
21. J. P. Kottmann, O. J. F. Martin, D. R. Smith, and S. Schultz, "Non-regularly shaped plasmon resonant nanoparticles as localized light source for near-field microscopy," *J. Microsc.* **202**, 60-65 (2001).
22. C. Girard, J.-C. Weeber, A. Dereux, O.J.F. Martin, and J.-P. Goudonnet "Optical magnetic near-field around nanometer-scale surface structures," *Phys. Rev. B* **55**, 16487-16497 (1997).
23. B. T. Draine, "The discrete dipole approximation and its application to interstellar graphite grains," *Astrophys. J.* **333**, 848-872 (1988).
24. J. P. Kottmann, O.J.F. Martin, D.R. Smith and S. Schultz, "Field polarization and polarization charge distributions in plasmon resonant particles," *New J. Physics* **2**, 27.1-27.9 (2000).
25. J. P. Kottmann, and O.J.F. Martin, "Plasmon resonant coupling in metallic nanowires," *Opt. Express* **8**, 655-663 (2001).
26. C. Girard, and S. Maghezzi, "Dispersion forces between a spherical probe tip and a periodic crystal: study of different asymptotic cases", *Surf. Sci.* **255**, L571-L578 (1991).

## 1. Introduction

Localized surface plasmons are electromagnetic modes associated to subwavelength metallic objects which result from the resonant coupling between the surface charge density and the light scattered by the object [1]. If the illumination is tuned to the resonant wavelength, the light is strongly enhanced and confined near the particle, where it can reach several hundred times the incident field amplitude [2]. When two metallic nano-objects are approached together, the individual modes are combined into collective modes with shifted wavelengths. The evolution of this mode structure with the distance is complex and strongly depends on the nature of the particles. For example, a field enhancement factor of several thousand can be observed in the gap between a small gold particle and an extended gold film [3].

Since the first work of Ashkin [4], it is well known that a light beam can exchange momentum with a micron-sized particle. The resulting force is usually decomposed into the so-called scattering and gradient forces. This seminal work opened the way for the realization of optical tweezers and the manipulation of a wide range of particles, from atoms to biological cells [5-8].

Manipulating particles on a nanoscale has always attracted a lot of interest and is key to a variety of applications. In this context, the use of evanescent waves is of primary interest as it allows very short spatial lengthscales and highly confined trapping geometries. For this reason, several theoretical studies have been carried out to further our understanding of the physical mechanisms responsible for optical forces in confined geometries. Typical model systems are dielectric or metallic particles near interfaces [9, 10], dielectric waveguides deposited on silica surface [11], particles in waveguides [12], or manipulation of dielectric

particles with optical forces created by a metallic tip [13, 14]. Moreover, it has been shown that metallic and dielectric particles behave very differently. In particular, the sign of the scattering force experienced by a plasmonic metallic particle strongly depends whether the system is excited at a wavelength close to that of the surface plasmon [15].

Recently, a study of the interaction between two silver nanowires has been published [16]. This article focuses on very short distances between the nanowires, where strong enhancement of the optical forces occurs. Another study concentrates on the optical forces within silver nanoparticle dimers and trimers deposited on a glass substrate [17]. In the present publication, we considerably extend the interaction range addressed in Ref. [16] and show that noticeable effects appear even at large separation distances. The paper is organized as follows: The first section presents the theoretical tools used for the simulation. The field is computed with the Green's tensor method, the forces are calculated with the Maxwell stress tensor. In the second section, the results of the simulations are extensively discussed within two interaction regimes: First the near-field coupling regime, in which the two nanowires interact through their scattered evanescent field. This regime is characterized by strong optical forces between the nanowires. Second the far-field coupling regime, where the two particles interact radiatively through their diffracted fields. Equilibrium positions between the particles in the center of mass reference frame are then discussed. A conclusion is given in the last section.

## 2. Model

The simplest configuration to investigate the optical forces between plasmonic nanoparticles is a two-dimensional geometry, with illumination in the plane of symmetry (Fig. 1). The two gold nanowires have a rectangular section ( $50 \times 110 \text{ nm}^2$ ) and are illuminated by a plane wave propagating along  $x$ -direction with propagation vector  $\mathbf{k}_i$  and incident electric field  $\mathbf{E}_i$  (Fig. 1). The experimental data of Johnson and Christy are used for the permittivity  $\varepsilon(\lambda)$  of gold as a function of the wavelength  $\lambda$  [18]; the scatterers are in vacuum. A key parameter for this study is the spacing  $d$  between the two particles.

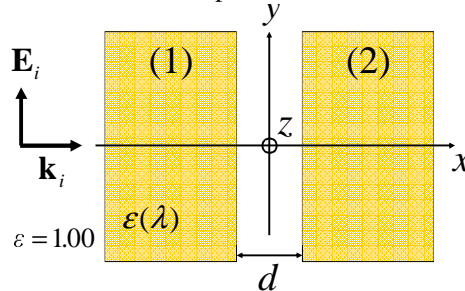


Fig. 1. Geometry of the system: two gold nanowires with the same rectangular section and a separation distance  $d$  are illuminated with a plane wave propagating in  $\mathbf{k}_i$  direction with incident field  $\mathbf{E}_i$ .

The Maxwell stress tensor is used to obtain the electromagnetic force on one or the other particle for a given illumination [19]. This requires the knowledge of the total electric and magnetic fields at the vicinity of the particle. The electric field  $\mathbf{E}$  is computed using the Green's tensor method described in Refs. [20, 21]. The magnetic field  $\mathbf{H}$  is then deduced from the electric field  $\mathbf{E}$  using the Maxwell-Faraday relation [22]. Let us emphasize that the validity and accuracy of the magnetic field and force calculations have been carefully checked. The extinction cross-section  $C_{ext}$  of the entire system, which corresponds to the sum of the absorption and scattering cross-sections, is also computed from the electric field [23].

Since the system has one invariance direction, we obtain a force  $\mathbf{f}$  per unit length. To normalize this force, we consider a square with the same area  $S_{ref}$  than the section of one wire and define the reference length  $L_{ref} = \sqrt{S_{ref}}$ . The radiation pressure  $p_{rad}$  created by entirely reflecting the incident field  $\mathbf{E}_i$  is then computed and the reference force  $\mathbf{f}_{rad}$  defined as:

$$\mathbf{f}_{rad} = p_{rad} L_{ref} \mathbf{x}, \quad (1)$$

where

$$p_{rad} = \varepsilon_o E_i^2, \quad (2)$$

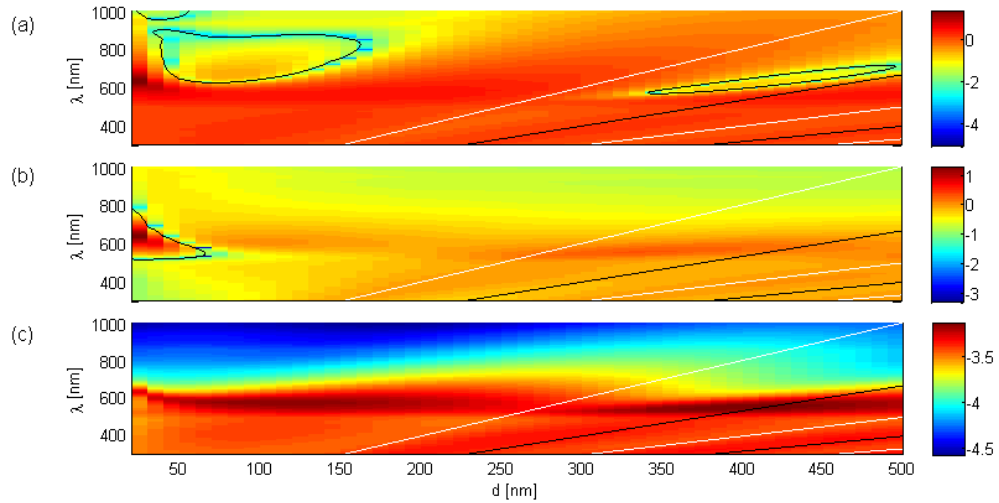
and  $\mathbf{x}$  is the unit coordinate vector and  $\varepsilon_o$  the vacuum permittivity. The normalized electromagnetic force is finally obtained as:

$$\mathbf{F} = \frac{\mathbf{f}}{f_{rad}}. \quad (3)$$

Since the incident light propagates parallel to a symmetry axis of the system, the force has no components along the  $y$ -direction. Hence, in the following, force will always refer to the  $x$ -component of the vectorial force normalized with Eq. (3).

### 3. Results

Figure 2 shows the force on each particle and the extinction of the entire system, in a logarithmic color scale as a function of the spacing  $d$  and illumination wavelength  $\lambda$ . To clarify the evolution of the system with the spacing, we separate the near field coupling region [Fig. 2 (a), (b) and (c)] and the far field coupling region [Fig. 2 (d), (e) and (f)].



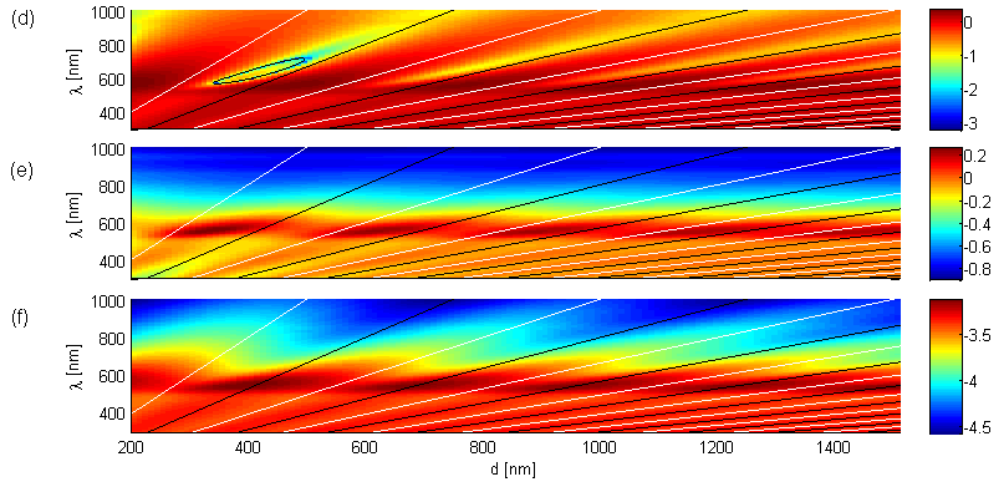


Fig. 2. (a, d). Optical force on particle (1) and (b, e): optical force on particle (2) as a function of the separation distance  $d$  and the wavelength  $\lambda$  in the near field coupling regime (a, b, c) and in the far field coupling regime (d, e, f). (c, f): extinction for the complete system. A logarithmic colorscale is used for all maps and the absolute value of the forces is shown.

Notice in Fig. 2 that the logarithmic scale requires to show the absolute value of the forces, which implies that the information on the sign of the forces is lost. Hence, black contours in Fig. 2(a,b,d,e), where the amplitude of the corresponding force vanishes, indicate a change in the sign of the force. In the near field coupling regime the force  $\mathbf{F}_1$  on the first particle is always positive except in the three regions limited by the black contours, Fig. 2(a). Also the force  $\mathbf{F}_2$  on the second particle is always positive except inside the black contour, Fig. 2(b). To evidence the different interaction regimes between both particles, we report in Fig. 3 these different contours, in blue for  $F_1 = 0$  and in red for  $F_2 = 0$ .

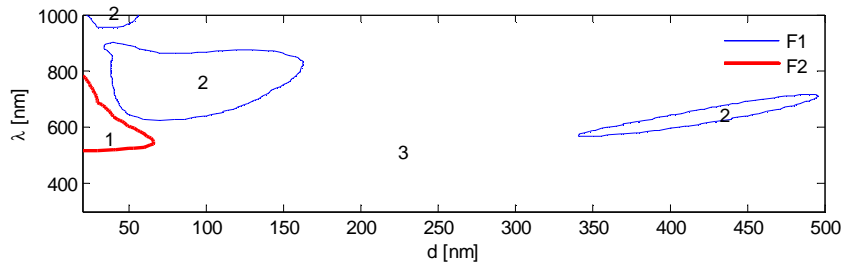


Fig. 3. The regions (1) (2) and (3) formed by blue and red contours determine the three possible interaction regimes between both nanowires as a function of the distance  $d$  and the wavelength  $\lambda$ : (1) Attractive forces, (2) Repulsive forces, (3) Positive forces.

Since the four regions enclosed by these contours do not overlap, no equilibrium positions with stationary particles exist. Three different forces configurations, labelled 1-3, are observed in Fig. 3:

- Inside the region (1),  $F_1 > 0$  and  $F_2 < 0$ , the forces between both particles are attractive.

- Inside the regions (2),  $F_1 < 0$  and  $F_2 > 0$ , the forces between both particles are repulsive.
- Inside the region (3),  $F_1 > 0$  and  $F_2 > 0$ , both particles are pushed by the illumination field.

Figure 3 indicates that these three different forces configurations are present in the near field coupling regime. Furthermore, only in this regime, attractive forces can be created: at distances smaller than 70 nm and for wavelengths  $515 \text{ nm} < \lambda < 785 \text{ nm}$ . At wavelengths larger than 625 nm, repulsive forces can be generated for the near field coupling regime as well as for the far field coupling regime. Finally, let us note that for all wavelengths  $\lambda < 515 \text{ nm}$ , forces on both nanowires are always positives and oriented along the illumination direction.

For small distances ( $d < 70 \text{ nm}$ ) and for  $550 \text{ nm} < \lambda < 730 \text{ nm}$ , we notice in Figs. 2(a) and (b) a region where both forces are strongly amplified and have opposite directions ( $F_1 > 0$  and  $F_2 < 0$ ). In fact, for these values of  $d$  and  $\lambda$ , it is possible to excite a plasmonic mode which gives rise to attractive forces. The extinction is also enhanced in this region, Fig. 2(c). However, the behaviour of the extinction remains usually quite different from that of the forces: For distances larger than 70 nm and around the wavelength  $\lambda = 560 \text{ nm}$ , the extinction increases – corresponding to the plasmon resonance of the system – but this enhancement is not visible on force maps. The correlation between plasmon resonances and enhanced optical forces is therefore quite subtle in such a coupled system.

Between the near field and the far field regimes, there is a transition zone which cannot be defined very precisely, where both particles are pushed along by the illumination field. In the far field coupling regime, Fig. 2(d)-(f), the forces are always positive except for that on the first particle inside the black contour in Fig. 2(d). In this case, the forces between the two nanowires are repulsive. In any other case, the force due to the radiation pressure dominates and both particles are pushed along by the incident field.

Figure 2 indicates a very different behaviour in the near field and in the far field coupling regimes; let us discuss them in greater detail in the following two sections.

### 3.1 Near field coupling regime

Figure 4 shows the enhancement of the forces and of the extinction as a function of the wavelength for three different separation distances ( $d = 10, 20$  and  $30 \text{ nm}$ ). The solid lines represent the force on the first particle whereas the dashed lines represent the force on the second particle.

Figure 4(a) shows that the force on the particle (1) is always positive, while that on particle (2) is negative for  $520 \text{ nm} < \lambda < 730 \text{ nm}$ . Thus, in this region, the forces between the two nanowires are attractive. The curves are quite symmetrical and both forces reach their maximum amplitude at the same wavelength. Moreover, if we compare the force and the extinction spectra, we observe that the forces reach their extrema close to the maximum extinction. For example, for  $d = 10 \text{ nm}$ , the extinction maximum is at  $\lambda = 720 \text{ nm}$  and the force extremum at  $\lambda = 730 \text{ nm}$ .

On the other hand, while the forces show only one maximum, the extinction has two maxima, corresponding to the two resonant plasmonic modes of this system; on the extinction curve, the mode at large wavelength is approximately 1.5 times larger than the other one and produces an attractive force  $F_{rad} \simeq 100$  for a separation  $d = 10 \text{ nm}$  whereas the force created by the other mode is insignificant.

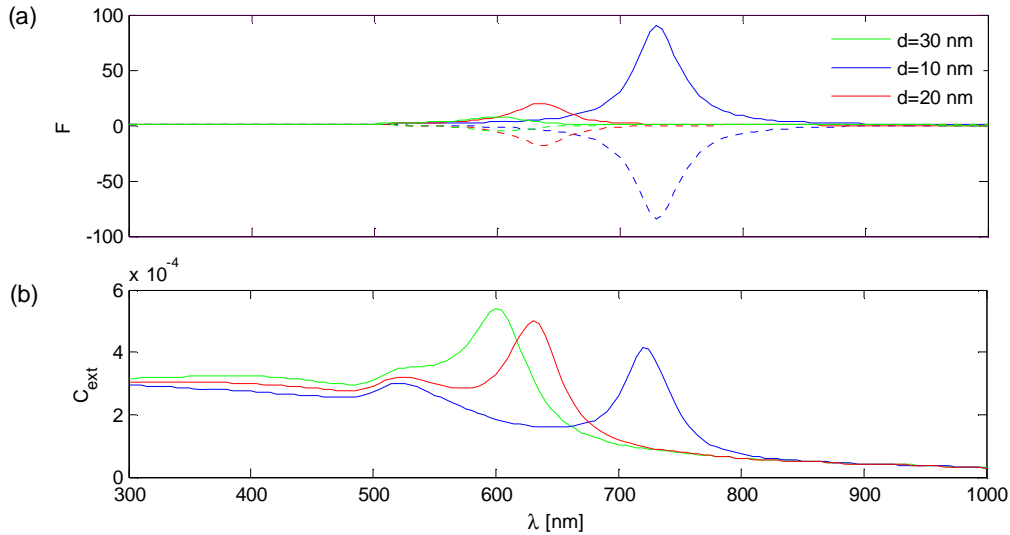


Fig. 4. (a) Forces on particle 1 (solid lines) and 2 (dashed lines) and (b) extinction spectra for three distances  $d$  in the near field coupling regime.

These two plasmonic modes correspond to two different modes of the coupled particles, with induced dipoles parallel to the long, respectively short sides of the particle. This is revealed by the field distribution at the vicinity of the particles, as sketched in Fig. 5. The resonance at large wavelength results from an antisymmetric combination of the two long-edge dipoles [Fig. 5(a)]. This coupling is non radiative and the energy is located mainly between the two particles, with opposite sign polarization charge densities on the gap [24, 25], resulting into an attractive force.

The other resonance visible in the extinction curve does not produce a force, Fig. 4(b). For this coupling mode, both particles are polarized in the same direction along  $x$ -axis and the system behaves globally as one single dipole [see Fig. 5(b)].

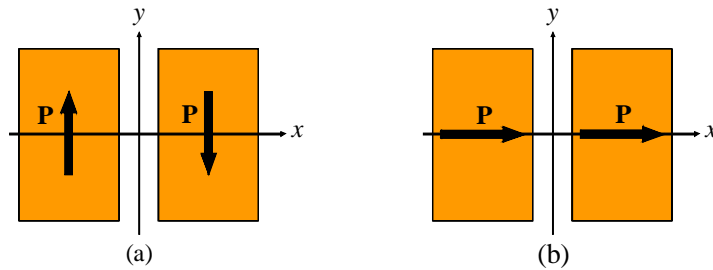


Fig. 5. Two coupling modes between both particles: (a) Antisymmetrical combination of both dipoles; this mode is non-radiative and produces a strong optical force. (b) Both particles are polarised along the incident field and no forces are observed.

To gain further understanding in the coupling phenomena in this system, Fig. 6 shows the position of the resonance wavelength  $\lambda$ , the corresponding forces  $\mathbf{F}_1$  and  $\mathbf{F}_2$ , and the extinction as a function of the distance  $d$ . The resonance wavelengths are computed from the force and from the extinction spectrum of the entire system.

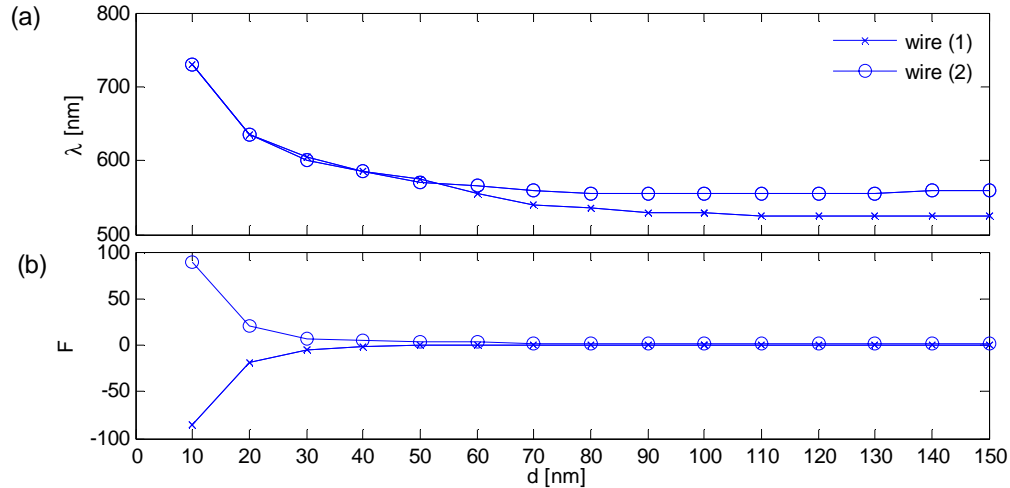


Fig. 6. (a) Resonance wavelength and (b) forces amplitude at the resonance for each particle, as a function of the separation distance  $d$ .

Figure 6(a) indicates that the resonance wavelength is blue shifted when  $d$  increases up to 80 nm. For large distances, the resonance wavelength for the first nanowire resonance reaches the asymptotic value  $\lambda \cong 550$  nm, which is 15 nm larger than the resonant wavelength of one isolated particle ( $\lambda = 535$  nm). For the second nanowire the asymptotic value is smaller: about  $\lambda = 525$  nm. Note that for distances  $d$  smaller than 60 nm, the two curves are superimposed since the system is now strongly coupled.

Figure 6(b) illustrates the rapid decay of the force with the distance. For a distance  $d$  varying from 10 nm to 30 nm, the normalised force decreases by a factor of 92%. The amplitude of the forces decreases until  $d = 60$  nm (corresponding to the edge of region 1 in Fig. 3). Then, the forces reach  $2.4 F_{rad}$  for the first particle and  $2.3 F_{rad}$  for the second.

### 3.2 Far field coupling regime

Let us now turn to the far field regime, as shown in Figs. 2(d)-(f). In these three graphs we observe in the spectral band  $520 \text{ nm} < \lambda < 570 \text{ nm}$  the presence of maxima occurring periodically with the spacing  $d$ . This periodicity is due to the cavity effect that takes place between the two particles. As a matter of fact, the modes of an ideal Fabry-Perot resonator are given by:

$$\lambda_n = \frac{2d}{n + \alpha}, \quad (4)$$

where  $\lambda_n$  is the modal wavelength of mode  $n=1,2,3,\dots$  and  $\alpha = \varphi / 2\pi$ , where  $\varphi$  is the phase between the incident wave and the wave reflected by the particle.

These modes are also shown in Fig. 2: the black lines correspond to  $\alpha = 0$  and the white lines to  $\alpha = 0.5$ . Note that the extinction maxima coincide with the modes of the Fabry-Perot resonator for  $\alpha = 0.5$ . However, the forces maxima are shifted from the Fabry-Perot modes. The study of the spectrum at constant distances will allow us to analyze these cavity effects and their consequences on the forces and the extinction.

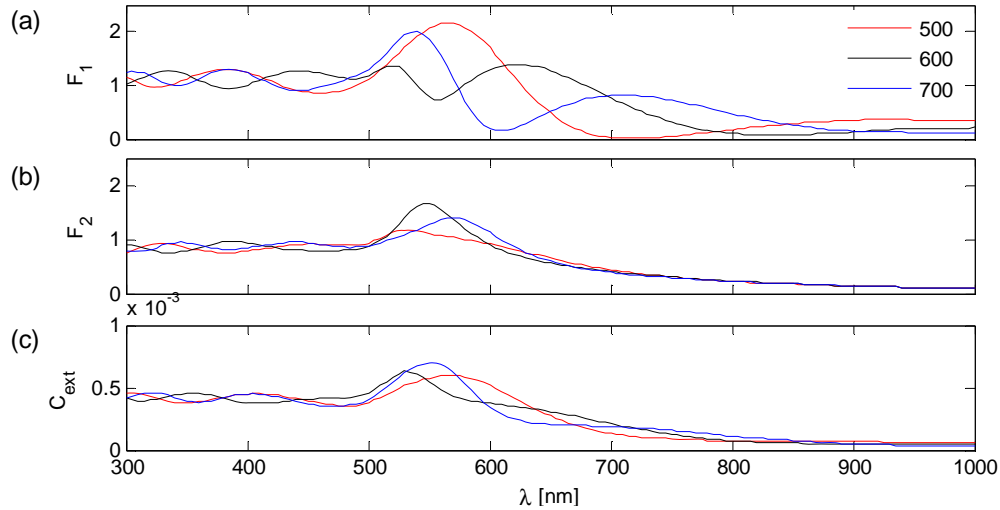


Fig. 7. (a) Forces on particle 1 and (b) particle 2, and extinction spectra for three distances  $d$ .

The forces and extinction spectra are shown in Fig. 7 for three separations  $d=500, 600$  and  $700\text{nm}$ , where the forces are always positive. We observe a main maximum around the plasmon resonance wavelength of an isolated particle  $\lambda = 550\text{ nm}$  and a secondary maximum at shorter wavelengths. For  $\lambda < 500\text{ nm}$ , we notice on forces and extinction spectra a sinusoidal oscillation, which corresponds to the cavity modes. However, for wavelengths larger than the plasmon resonance, this modulation vanishes. Hence, the response of the system results from the interaction of the cavity modes with the plasmon mode.

Lets us now analyze the evolution of the forces and the extinction as a function of the separation  $d$  for a wavelength  $\lambda = 550\text{ nm}$  situated close to the plasmon resonance (Fig. 8).

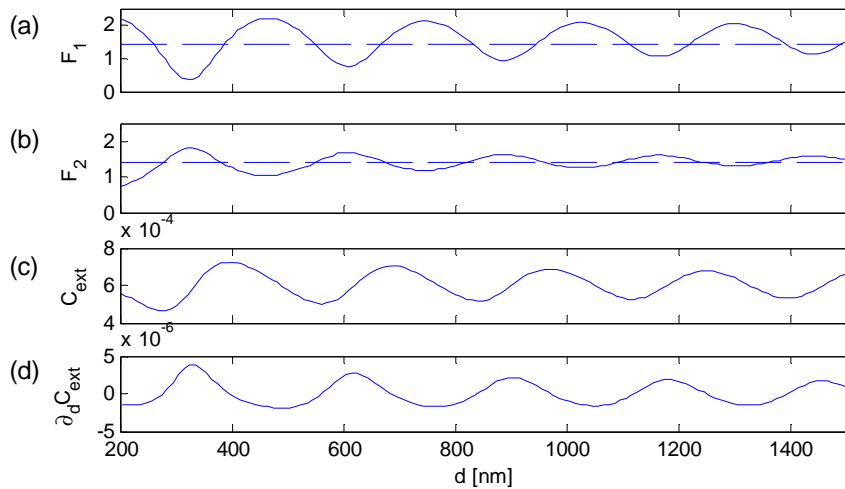


Fig. 8. (a) Forces on particle 1 and (b) particle 2; (c) extinction spectra and (d) derivative of the extinction, as a function of the distance  $d$  at the plasmon resonance wavelength  $\lambda = 550\text{ nm}$ .

At first hand, we can observe the sinusoidal modulation of the forces and extinction due to the resonant modes of the cavity, Figs. 8(a)-(c). The oscillation periods ( $282.5\text{ nm}$  for  $F_1$  and  $277.5\text{ nm}$  for  $F_2$ ) are larger than half the plasmon resonance wavelength of an isolated

particle ( $\lambda_{sp}/2=267.5\text{ nm}$ ) but their average is similar to the period of the extinction:  $280\text{ nm}$ . The forces average, indicated by dashed horizontal lines in Fig. 8(a) and (b), is situated around 1.4. When the separation distance  $d$  increases, the forces converge to the same average value, equal to the value of the radiation pressure exerted by the incident field on each particle individually.

Let us note quadrature phase shifts between the forces and the extinction maxima. The variation of the extinction as a function of the distance will allow us to explain this shift. Indeed, in a first approximation, it is possible to decompose the force into two contributions: a radiation force due to the radiation pressure of the incident field and a gradient force depending on the gradient intensity along the illumination direction. The extinction is expected to evolve roughly proportionally to the average field inside the particle; hence its derivative provides information on the gradient force contribution on the particles. Figure 8(d) shows that the maxima and minima of the derivative of the extinction with respect to the distance  $d$  coincide indeed with the maxima and minima of the forces, compare Fig. 8(a), (b) and (d). Thus, the force amplitudes depend on the intensity distribution inside the cavity. When the cavity is tuned to the illumination wavelength, the field is maximal, the intensity derivative with respect to the particle position is minimal, and the gradient force is zero. Hence, the forces  $F_1$  and  $F_2$  are close to their average value corresponding to the radiation pressure of the incident field. On the other hand, when the cavity is not tuned to the incident wavelength, the intensity gradient does not vanish and the gradient force contribution is added to or subtracted from the radiation force.

In summary – in a first approximation – the absolute value of the force gradient is maximal when the electric field gradient is maximal, namely when the absolute value of the extinction derivative is maximal.

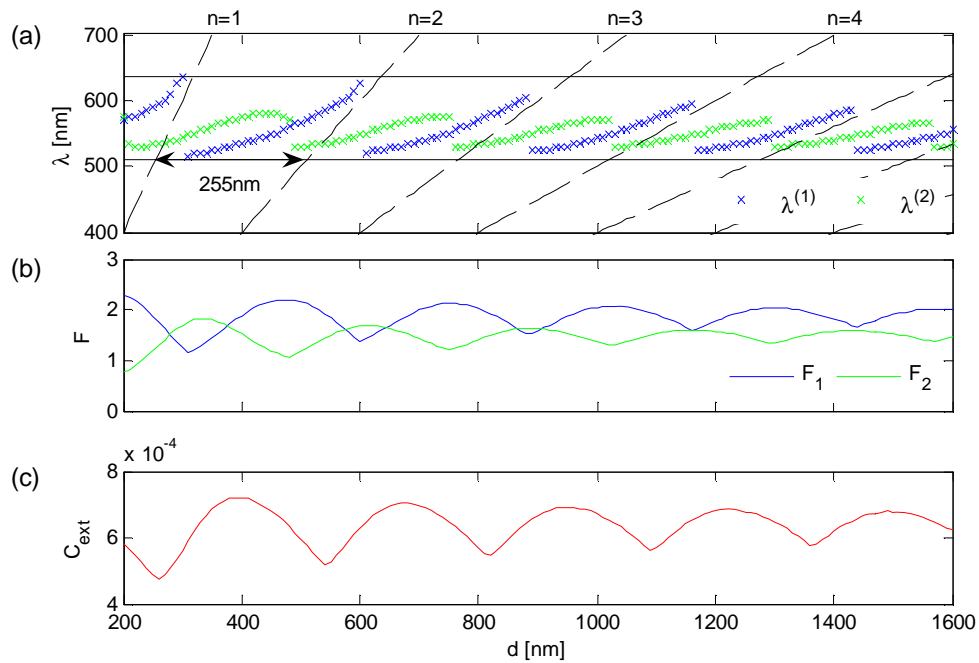


Fig. 9. (a) Evolution of force resonance wavelengths (b) force amplitudes and (c) extinction as a function of the separation distance  $d$ .

Let us now examine the behaviour of this coupled system as a function of the distance  $d$  at the plasmon resonance wavelength. Figure 9 illustrates the wavelength evolution of the  $F_1$  and  $F_2$  maxima and the amplitude evolution of both forces and extinction.

Figure 9(a) represents the evolution of the resonance wavelengths  $\lambda^{(1)}$  and  $\lambda^{(2)}$  for both forces as a function of the distance  $d$  (the resonance wavelength is determined by the force maximum, see e.g. Fig. 7). The blue colour is attributed to particle (1), the green colour to particle (2). Dashed black lines have been added; they correspond to the modal wavelengths  $\lambda_n$  of an ideal Fabry-Perot resonator with  $\alpha = 0$ , Eq. (4).

The  $\lambda_n$  straight lines stress three properties of the Fabry-Perot resonator. First, the  $\lambda_n(d)$  slope  $2/n + \alpha$  decreases when the mode number  $n$  increases. Second, the straight lines  $\lambda_n$  intercept lines  $\lambda = cst$  at regular intervals, for example at  $\lambda = 510$  nm the intervals are equal to 255 nm, Fig. 9(a). Third, all lines  $\lambda_n$  cross the origin (not visible in Fig. 9). Some of these characteristics are reproduced in the behaviour of  $\lambda^{(1)}$  and  $\lambda^{(2)}$ : For each cavity mode,  $\lambda^{(1)}$  follows the lower wavelength boundary for small separations  $d$  and tends toward the corresponding Fabry-Perot mode  $\lambda_n$  for larger separations, Fig. 9(a). The  $\lambda^{(2)}$  average slope decreases when the mode number increases; though its value is smaller than the corresponding Fabry-Perot mode.

Furthermore, these numerical lines do not intercept the origin but converge towards the value  $\lambda \approx 510$  nm which was already observed in Fig. 2. Thus, the interaction between Fabry-Perot modes and plasmon resonances results in a mixed mode with displaced wavelength. The wavelength band observed in Fig. 9(a) has a width of  $\Delta\lambda = 125$  nm and is centred around  $\lambda \approx 550$  nm which is close to the plasmon resonance wavelength of an isolated particle. These results indicate that the modes of the Fabry-Perot cavity formed by the two particles are filtered by the plasmon resonance of the system.

The forces and extinction maxima shown in Fig. 9(b) and (c) exhibit a similar behaviour to that discussed in Fig. 8. In particular, we recognize the periodicity of 270 nm which corresponds approximately to half the surface plasmon wavelength. Forces maxima are in quadrature phase shift with extinction maxima. This shift results again from the gradient force contribution which depends on the resonant degree of the cavity. Hence, forces and extinction oscillate around a constant value when the quality of the cavity is changed. When the separation increases, the coupling interaction decreases and the forces as well as the extinction diminish until they reach the values corresponding to that of one isolated nanowire.

### 3.3 Equilibrium positions

A very interesting question for the practical utilisation of such coupled system is whether stable "molecules" can be formed by illuminating two individual plasmonic particles. To address this question, we study here the optical forces in the centre of mass reference frame (CMRF) for the far field coupling regime. Lets us recall that in this far field coupling regime, optical forces push both particles along the illumination direction. The total force  $\mathbf{F}_T = \mathbf{F}_1 + \mathbf{F}_2$  on the centre of mass is parallel to the  $x$ -axis and positive. However, because of system symmetry, the force applied on particle (2) in the CMRF is simply given by the difference  $2\mathbf{F}_{CM} = \mathbf{F}_2 - \mathbf{F}_1$  and inversely the quantity  $-2\mathbf{F}_{CM} = \mathbf{F}_1 - \mathbf{F}_2$  corresponds to the force applied on particle (1). To analyze the equilibrium positions as a function of the separation distance  $d$ , three cases must be considered:

- $F_{CM} < 0$     The particles attract each other.
- $F_{CM} = 0$     Equilibrium condition in the CMRF.

- $F_{CM} > 0$  The particles are repulsed.

Figure 10 shows  $F_{CM}$  as a function of the wavelength  $\lambda$  and the distance  $d$ . As previously observed for the force maps in Figs. 2 (d) and (e), we recover here on the force difference  $F_{CM}$  the periodicity due to the cavity mode as a function of the distance  $d$  (Fig. 10). The black contours in Fig. 11 indicate equilibrium positions where the condition  $F_{CM} = 0$  is satisfied. Note that equilibrium positions cover the entire wavelength range and thus it is always possible to find at least one equilibrium wavelength for any given distance  $d$ . Inside these contours  $F_{CM}$  is negative and positive outside. Hence, both particles are attracted within the black contours and repulsed outside.

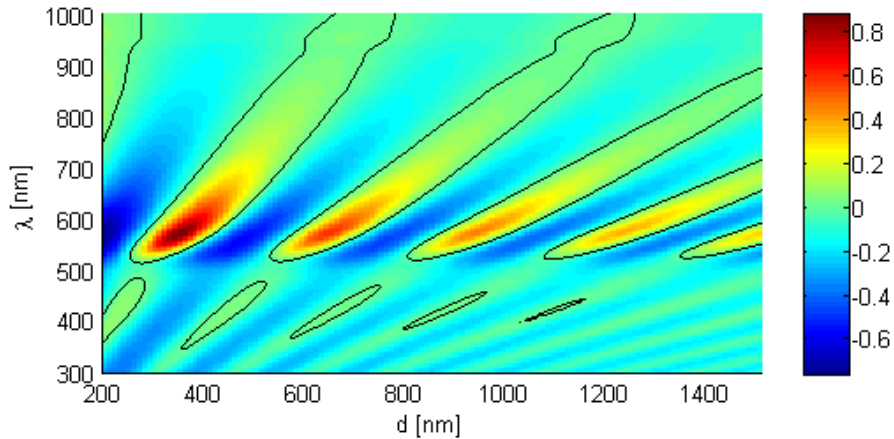


Fig. 10. Force applied on wire (2) in the centre of mass reference frame as a function of the separation distance  $d$  and the wavelength  $\lambda$ . Black contours represent the equilibrium positions of the system.

Afresh, as a function of the distance, we note periodic maxima around the plasmon resonance wavelength but their amplitude decreases with the distance. To gain further understanding, let us now consider a constant wavelength  $\lambda = 550$  nm close to the plasmon resonance.

Figure 11 shows the evolution of  $F_{CM}$  as a function of the separation  $d$ , for  $\lambda = 550$  nm; the extinction  $C_{ext}$  and its derivative  $\partial_d C_{ext}$  are also shown in this figure. The force  $F_{CM}$  exhibits a sinusoidal periodicity with  $d$ , Fig. 11 (a). The force value  $F_{CM}$  oscillates around zero while its amplitude is limited by  $\pm 0.75 F_{rad}$  and decreases with the distance. The  $F_{CM}$  maxima and minima coincide with the extinction derivative maxima and minima in the same manner as was previously observed in Fig. 8 for  $F_1$  and  $F_2$ . This again results from the gradient force, which is maximal or minimal when the derivative of the extinction is maximal or minimal. The order of magnitude for the potential depth can be estimated by approximating the oscillation of the force around  $d = 1 \mu\text{m}$  and considering 100 nm thick particles. This leads to a  $24 \text{ meV} = 1 \text{ k}_B\text{T}$  potential depth for a  $5 \text{ mW}/\mu\text{m}^2$  laser power at  $T=293 \text{ K}$ .

The separation distances  $d_o$  for which  $F_{CM}$  is equal to zero correspond to the equilibrium positions. They represent stable equilibrium positions when they are located on the negative slope of the  $F_{CM}$  curves and unstable equilibrium when they are on the positive

slope, Fig. 11(a). For the former, a small variation  $\Delta d$  around the equilibrium position situated on the negative slope produces a force  $F_{CM}$  which tends to bring the particle back to the equilibrium position and conversely for the unstable equilibrium positions.

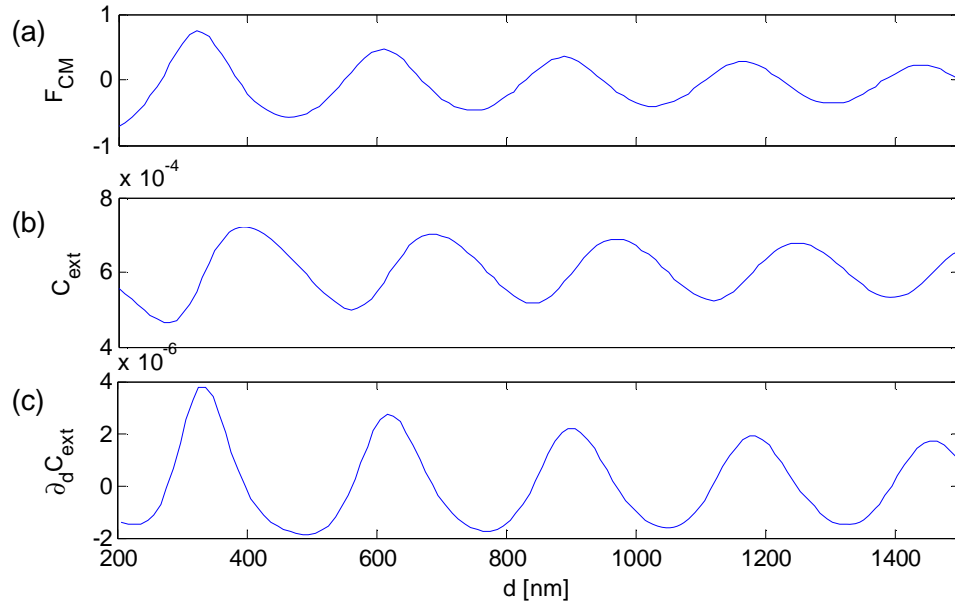


Fig. 11. (a) Force on particle (2) in the centre of mass reference frame at the plasmon resonance wavelength, (b) extinction and (c) extinction derivative, as a function of the separation distance  $d$ . Equilibrium positions  $F_{CM} = 0$  are stable on the decreasing sides of the curve and unstable on the increasing sides.

The van der Waals interaction between the two wires was not taken into account in this study for the following reason: The amplitude of the van der Waals interaction can be very large at very short distances (from angstrom to a few nanometers), and reach easily several piconewtons. In the system under study, this interaction cumulates with the optical force around the plasmon resonance (both are attractive). Moreover, the force for a distance of 10 nm reaches one hundred times the equivalent radiation pressure due to the excitation of the surface mode and is then larger than van der Waals interaction for a typical laser power. For large distances, the van der Waals interaction becomes negligible [26].

#### 4. Conclusion

We have studied the forces created on two coupled gold nanowires when they are illuminated at the plasmon resonance wavelength. Three different forces regimes have been observed: attractive forces, repulsive forces and parallel forces pointing in the same direction. These three regimes, which depend on the excitation wavelength and on the separation distance between both particles, are observed in the near-field coupling regime. The attractive forces, which lead to the creation of a light-induced "molecule", are only generated at the plasmon resonance wavelength or close to it. Their magnitude can exceed 100 times the force due to the radiation pressure.

In the far field coupling regime, the radiation pressure dominates and both nanowires are pushed by the incident field, while their interaction leads to a modulation of the force experienced by each particle. The system behaves then as a cavity, where the plasmon resonances interact with the modes of the cavity. When the cavity is tuned to the incident wavelength the forces experienced by the particles are close to their average value. On the

other hand, periodical forces maxima and minima are observed as a function of the separation distance when the cavity is detuned. In this case, the force on the first particle takes its maximum when the force on the second one is minimum, and conversely. At first approximation, we can say that the force amplitude is the sum of the radiation pressure due to the incident field modulated by the gradient force at the location of the particle.

Finally, in the far field coupling regime and in the centre of mass reference frame, it is possible to find at least one equilibrium position for any wavelength. At a fixed wavelength close to the plasmon resonance, alternative stable and unstable equilibrium positions are periodically observed as a function of the separation distance  $d$  between the wires. The electromagnetic forces on each object are identical at these equilibrium positions.

The different forces regimes investigated in this paper can be useful to build nanosystems, where the optical forces are utilized to bind, repel, or manipulate metallic particles for a broad variety of applications.

### **Acknowledgements**

It is a pleasure to acknowledge stimulating discussion with A. Dereux, J.M. Fournier, R. Gómez-Medina, L. Huang, and P. Jacquot. This work was supported in part by the European Network of Excellence Plasmo-nano-devices (contract FP6-2002-IST-1-507879).